

Proposed Effective Width Criteria for Composite Bridge Girders

Stuart S. Chen¹; Amjad J. Aref²; Methee Chiewanichakorn³; and Il-Sang Ahn⁴

Abstract: In a composite section, in-plane shear strain in the slab (acting as a flange in the composite girder) under the applied bending causes the longitudinal displacements in the parts of the slab remote from the webs to lag behind those near the webs. This phenomenon, termed *shear-lag*, can result in an incorrect calculation of the displacement and extreme fiber stresses when using only the elementary theory of beam bending. The *effective width* concept has been introduced, widely recognized, and implemented into different codes of practice around the world as a simplified practical method for design and evaluation of structural strength and stiffness while accounting for shear-lag effects indirectly. Each code implements different ideas and approaches for specifying effective width. This paper proposes simpler and more versatile design criteria for computing the effective width (b_{eff}) in steel-concrete composite bridges. A parametric study was conducted based on finite-element analysis of bridges selected by a statistical method—namely, *design of experiment* concepts. Both simple-span and multiple-span continuous bridges were considered in the parametric study. The finite-element methodology was validated with companion experiments on 1/4- and 1/2-scale specimens. Effective width values at the critical sections were computed from stresses extracted from FEM models and used in developing candidate design equations. The final design criteria were selected based on assessment of impact of candidate equations. Use of full width—the most versatile, simplest, and sufficiently accurate effective width design criteria, is proposed for both positive and negative moment regions.

DOI: 10.1061/(ASCE)1084-0702(2007)12:3(325)

CE Database subject headings: Width; Shear lag; Design criteria; Bridge, girder; Bridges, composite; Steel; Concrete.

Introduction

In a composite section, in-plane shear strain in the slab (acting as a flange in the composite girder) under the applied bending causes the longitudinal displacements in the parts of the slab remote from the webs to lag behind those near the webs. This phenomenon was termed *shear-lag*. Shear-lag phenomenon can result in an incorrect or underestimated displacement and extreme fiber stresses when using only the elementary theory of beam bending. The concept of *effective width* was introduced for simplifying the analysis and design of the composite section (Moffatt and Dowling 1978).

The *effective width* concept has been widely recognized and implemented into different codes of practice around the world. This concept provides a simplified practical method for design

and evaluation of structural strength and stiffness while accounting for shear-lag effects indirectly. Each code implements different ideas and approaches for specifying effective width (Ahn et al. 2004). Heins and Fan (1976) used orthotropic plate governing equations in their study and concluded that the effective width in the 1973 AASHTO Specifications overestimated the effective width for the interior girders and underestimated effective widths for the exterior girders.

The current AASHTO provisions for composite beams stipulate that for an interior girder, except for orthotropic deck and segmental concrete structures, effective width be taken as the least of: (1) one-quarter of the effective span length; (2) 12.0 times the average depth of the slab plus the greater of web thickness or one-half the top flange width; and (3) the average spacing of adjacent beams. These provisions are archaic, originating from concrete T-beam design provisions which were co-opted when the “Standard Specifications for Highway Bridges” (AASHTO 1944) adopted the first provisions for composite beams. In the early 1900s, the effective width provisions for concrete T-beams were studied, resulting in several different formulations of effective width (Ferro-Concrete 1910; Committee 1916; ACI 1917; Goldbeck and Smith 1916; Unwin 1911; Waldram 1913). Based on other studies and engineering practices, the “Final Report of the Special Committee on Concrete and Reinforced Concrete” (Special 1916) introduced the provision of effective width of concrete T-beams as the minimum of one-fourth of the span length of the beam and twelve times the thickness of the slab. That provision has remained in place for 90 years.

Moffatt and Dowling (1978) used the finite-element method for developing effective flange width of box girder bridges. Their study was used as the basis for effective breadth rules in the British Specification (BSI 1979, 1982). Cheung and Chan (1978)

¹Associate Professor, Dept. of Civil Engineering, SUNY at Buffalo, Buffalo, NY 14260. E-mail: ciechen@eng.buffalo.edu

²Associate Professor, Dept. of Civil Engineering, SUNY at Buffalo, Buffalo, NY 14260. E-mail: aaref@eng.buffalo.edu

³Engineer, KPFF Consulting Engineers, 6080 Center Dr., Suite 300, Los Angeles, CA 90045; formerly, Post-Doctoral Research Associate, Dept. of Civil Engineering, SUNY at Buffalo, Buffalo, NY 14260. E-mail: mchiewanichakorn@kpff-la.com

⁴Postdoctoral Research Associate, Dept. of Civil Engineering, SUNY at Buffalo, Buffalo, NY 14260. E-mail: iahn@eng.buffalo.edu

Note. Discussion open until October 1, 2007. Separate discussions must be submitted for individual papers. To extend the closing date by one month, a written request must be filed with the ASCE Managing Editor. The manuscript for this paper was submitted for review and possible publication on August 31, 2005; approved on June 2, 2006. This paper is part of the *Journal of Bridge Engineering*, Vol. 12, No. 3, May 1, 2007. ©ASCE, ISSN 1084-0702/2007/3-325–338/\$25.00.

used finite strip methods to analyze realistic effective width for over 300 bridge models with Ontario highway bridge loadings and AASHTO HS-25 wheel loads. They found that for most practical bridges, girder size and deck thickness have very little effect on the effective width computations. Where full width is not effective, as the major contributing factors, they used span length and girder spacing. Subsequent versions of the Ontario Highway Bridge Design Code and the current Canadian bridge code have adopted their results for defining effective width of composite and concrete bridges (CSA 2000, 2001).

As far as limit states are concerned, shear-lag effects are not considered at the ultimate limit state in British Specifications (BSI 1979). In the current AASHTO-LRFD Bridge Design Specifications (2004), the same effective width is used for both service and strength limit states. The current Canadian Specifications also uses the same effective width for stress and capacity calculation (CSA 2000). Underestimation of effective width is conservative for the resistance of a beam, so this may be advantageous for simplicity of design, even though inaccurate. Simplicity of design is also the rationale for the use of elastic analysis for effective width evaluation with uncracked concrete, because effective widths are increased both by inelasticity and by cracking of concrete (Johnson and Anderson 1993).

The concept of effective width in positive moment regions has been investigated by many researchers (Adekola 1968; Daniels and Fisher 1966; Moffatt and Dowling 1978; Elhelbawey et al. 1999), while there is a limited amount of research focused on negative moment regions either analytically or experimentally (Viest and Siess 1953; Viest et al. 1958; Ansourian 1983). Nassif et al. (2005) conducted a parametric study based on finite-element analysis and found that where full width is not effective, the span length of the bridge and the girder spacing are the parameters most affecting effective width. However, the investigation only considered simple-span bridges.

Ahn et al. (2004) conducted comparative studies of the effective width provisions among national and international specifications. This study showed a similarity between EUROCODE 4 and AASHTO specifications when thickness limitation was neglected. In addition, the effective width computed based on AASHTO Specifications is conservative for some bridges, i.e., only those bridges whose girder spacings exceed the $12t_s$ limit, compared to the finite-element analysis results (Chiewanichakorn et al. 2004).

The objective of this study is to develop a more versatile yet simple design criteria for computing the effective width (b_{eff}) in steel-concrete composite bridges. The concept of effective width is very important for a simplified structural analysis, especially for computing stresses and displacements. Therefore, the accuracy of effective width has a major impact on the design of structural components.

Effective Width Definitions

Positive Moment Section

In a typical section under positive bending, the concrete slab is subjected to compressive stress and the majority of the steel section is under tensile stress. The neutral axis may be initially located in the steel section and migrate toward the slab as the applied moment increases. The neutral axis is often located either in the top flange of steel girder or concrete slab. Chiewanichakorn et al. (2004) proposed a new effective slab width definition for positive moment as

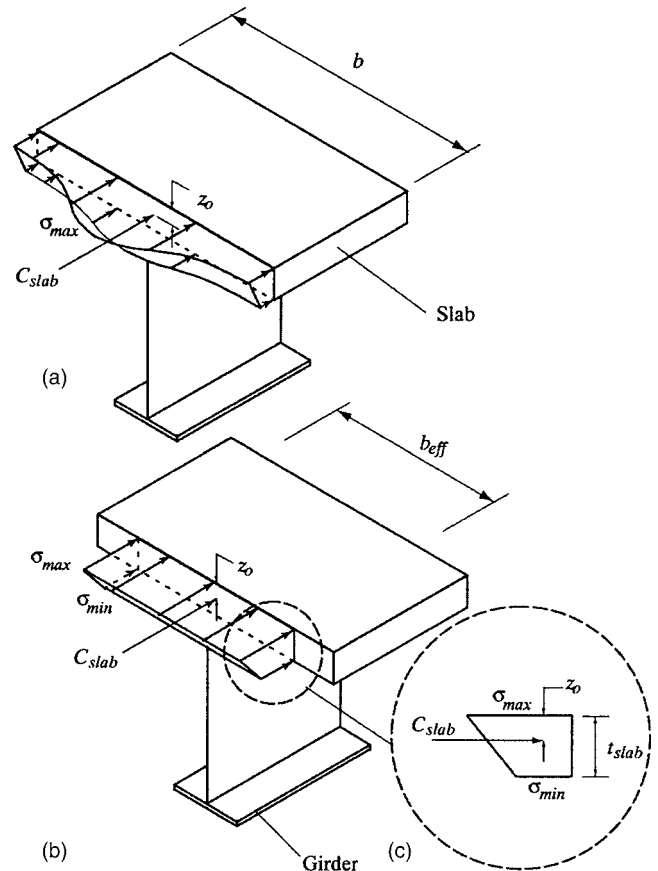


Fig. 1. Effective width definition (Chiewanichakorn 2005)

$$b_{eff} = \frac{C_{slab}}{F} = \frac{C_{slab}}{0.5t_{slab}(\sigma_{max} + \sigma_{min})} \quad (1)$$

where C_{slab} =total slab compressive force; F =force per unit slab width or the trapezoidal area of the stress block; t_{slab} =total slab thickness in compression; and σ_{max} and σ_{min} =maximum and minimum compressive slab stresses, respectively. This definition explicitly accounts for slab through-thickness stress variation, unlike the traditional definition. Fig. 1 illustrates the concepts associated with Eq. (1), where b denotes physical slab width and b_{eff} represents effective width.

Negative Moment Section

In multispan continuous bridges, the slab is subjected to tensile stresses in the region over the interior supports. Under negative moment, as soon as slab cracks initiate, concrete load is shed to longitudinal reinforcement and girder until the only deck forces acting are in the reinforcement after the slab is fully cracked. A definition analogous to the positive moment region one was developed based on the previous assumptions as shown in (Chiewanichakorn et al. 2005; Aref et al. 2006)

$$b_{eff} = \frac{T_{total}}{F} = \frac{T_{total}}{0.5t_{slab,t}(\sigma_{max} + \sigma_{min}) + T_{rebar_top} + T_{rebar_bot}} \quad (2)$$

where T_{total} =total tensile force from concrete and reinforcements; F =force per unit slab width or the trapezoidal area of the stress block; $t_{slab,t}$ =total slab thickness in tension; σ_{max} and σ_{min} =maximum and minimum tensile slab stresses, respectively;

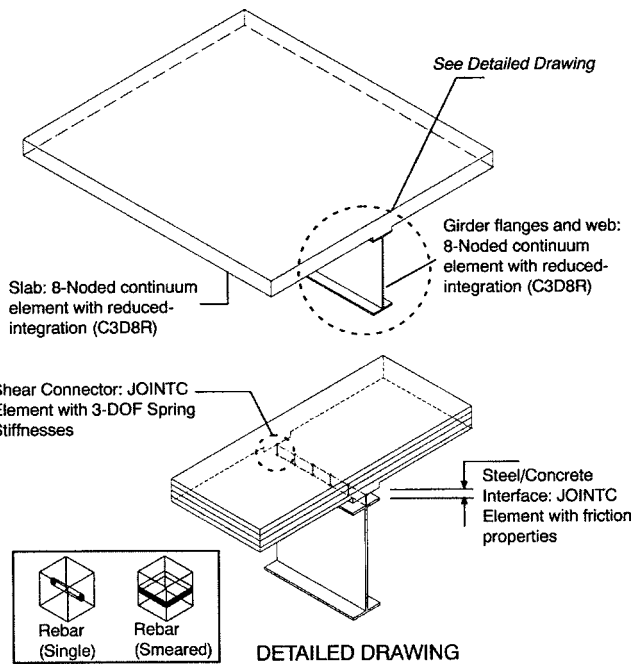


Fig. 2. Finite-element model of steel-concrete composite section (Chiewanichakorn 2005)

$T_{\text{rebar_top}}$ = force per unit width of top reinforcements; and
 $T_{\text{rebar_bot}}$ = force per unit width of the bottom reinforcements.

Finite-Element Modeling

A three-dimensional finite-element method was employed in this study (NCHRP 2005). Girder webs and flanges were modeled using eight-noded solid elements, namely, C3D8R in ABAQUS (HKS 2000). The concrete slab was modeled in a similar manner to girders using solid elements with finer meshes near a web-to-flange intersection in order to capture any shear-lag phenomenon and to fully capture the high stress gradient that occurs in this region. In addition, strain variation through the slab thickness could be monitored by having multiple layers of elements in slab. Steel reinforcements in the slab were modeled as smeared rebar using the REBAR option in ABAQUS (HKS 2000). Stiffness of the reinforcement is superposed onto the stiffness of the solid elements in which the reinforcement resides. By using this smeared rebar property in the reinforcement modeling, bond-slip effects are ignored.

Steel and reinforcement were modeled as elastic-perfectly plastic material in both tension and compression. Modulus of elasticity of 200 GPa was used for both web and flanges. In this study, an advanced ANAMAT concrete model (ANATECH Corp. 1997) was employed to model concrete deck material. The ANAMAT concrete constitutive model is based on smeared-cracking methodology and a Drucker-Prager modified J_2 -plasticity theory. In the ANAMAT concrete model, a crack is a mechanism that transforms the material from isotropic to orthotropic, where the material stiffness normal to the crack surfaces become zero, whereas the full stiffness parallel to the cracks is maintained.

Composite action between concrete slab and steel girder was modeled using a connector element called “flexible joint element”—JOINTC elements in ABAQUS. These elements are made up of three translational springs in a local coordinate

system. The JOINTC elements that represent the shear connectors in this study consist of three nonlinear springs, capturing all translational directions. An empirical formulation proposed by Oehlers and Coughlan (1986), which incorporates the beneficial effect of friction to augment the performance of the shear connector, was employed in modeling two orthogonal spring elements to simulate the shear stiffness of the shear connectors. The stiffness of the spring normal to the interface is computed as an axial stiffness based on the diameter and embedded length of the shear connectors. Fig. 2 shows schematic components of the finite-element model used in this study.

Validation of Finite-Element Model

The three-dimensional finite-element modeling described previously and further described in NCHRP (2005) was successfully verified with past experiments (Kathol et al. 1995; Daniels and Fisher 1966). The results show that the finite-element method (FEM) gives good representations of both global (force-displacement) and local behaviors (stresses and strains) compared to experimental results. Shear-lag phenomenon and strain variation through the slab thickness were well captured due to the nature of the three-dimensional model and its multiple layers of slab elements. In addition, this modeling method has been verified with the experiments conducted by the writers for both positive and negative moment sections (Ahn et al. 2005; NCHRP 2005).

Determination of Effective Widths

Effective widths of a section is determined herein from finite-element analysis results using Eqs. (1) and (2). For example, in a positive moment region section, the total slab compressive force (C_{slab}) is calculated as the sum of products of slab element stresses and cross-sectional areas of slab elements at that section. Total slab thickness in compression (t_{slab}) and maximum slab compressive stress (σ_{max}) can be directly obtained from finite-element analysis results. Based on these three variables, minimum slab compressive stress (σ_{min}) can be computed, and hence effective widths can be determined from Eq. (1). Effective widths in negative moment sections are computed in a similar manner using Eq. (2). This method is called an equilibrium-based approach proposed by Chiewanichakorn et al. (2004, 2005), as it is based on equilibrium of slab forces and of moments between the FEM model and the effective-width-based line girder: the same slab force resultant must occur in each, and the location of the resultant must be the same in each to produce the same moment, as shown in Fig. 1.

Design of Experiment Concepts

Design of experiments is a statistical method that is widely used in the general areas of product and process design, process improvement, and quality engineering. This method was specifically employed in this research to eliminate human bias in selecting variables that were considered to have major influences on effective widths, and therefore creating a viable statistical sample in a parametric study.

Experimentalists extensively use a strategy called a *one-factor-at-a-time* approach to enumerate cases based on multiple parameters. The method consists of choosing a baseline set of values (level) for each factor, then successively varying each

factor over a considered range while the other factors remain constant at the baseline level (Montgomery 2001). After all tests are performed, a series of plots are generated to demonstrate how each factor affects the results with all other factors held constant. Although this strategy is simple, it fails to consider possible interaction between the factors.

Factorial Design: The more appropriate approach to consider several factors is to conduct a *full factorial* experiment, an experimental strategy in which factors are simultaneously varied rather than *one-factor-at-a-time*. The effect of each factor or *main effect* as well as the interaction between factors can be quantitatively determined by a *regression model representation* (Montgomery 2001). For instance, the regression model representation of a two-factor factorial experiment can be expressed as

$$y = \beta_0 + \beta_1 x_1 + \beta_2 x_2 + \beta_{12} x_1 x_2 + \varepsilon \quad (3)$$

where y =response; x_1 and x_2 =independent variables; β =regression parameters; and ε =residual or error.

Let p be the number of factors (independent variables) and k be the number of levels considered for each factor. The total number of experiments required to satisfy the factorial design becomes p^k . For example, a complete replicate of a problem with two factors ($p=2$) and four levels ($k=4$) of each factor is 2^4 or 16 runs. As the number of factors increases, the number of runs required for the full factorial experiment rapidly outgrows the available resources. If the experimentalists can reasonably assume that certain high-order interactions are negligible, then information on the main effects and low-order interaction may be obtained by running only a fraction of the complete factorial experiment. This concept is called *fractional factorial design* (Goode 1999; Welch 2003). From the previous example, if the experimentalists cannot afford to run all 2^4 or 16 combinations perhaps they can, however, afford eight runs, one-half of a 2^3 design, which are eight cases. Using the concepts of the design of experiments and fractional factorial design, the number of analyses can be dramatically reduced by systematically selecting cases without affecting the results.

Parametric Study

The main purpose of conducting the parametric studies in this paper is to develop a sufficiently broad basis for simplified yet sufficiently accurate design equations to compute effective width. Based on the design of experiment concepts, both simple-span and multiple-span continuous bridges used in the parametric study were selected accordingly. A total of 240 analysis cases were considered for steel-concrete composite girders, considering both service and strength, both interior and exterior girders, and several cross sections in both positive and negative moment regions. Bridges with 2.4 m girder spacings were designed and modeled with decks 175 mm thick, those with 3.6 m girder spacings with decks 200 mm thick, and those with 4.8 m girder spacings with decks 240 mm thick.

Simple-Span Bridges

Three main parameters ($k=3$) for simple-span cases consisted of girder spacing (S), span length (L), and skew angle (θ). By considering two different levels ($p=2$) or values of each factor, i.e., low and high, a total number of factorial cases becomes $p^k=2^3=8$ bridge configurations. Intermediate values provide additional configuration(s).

Table 1. Simple-Span Parametric Study Cases

Bridge identification	Parameter			L/S
	S (m)	L (m)	θ (degrees)	
SS-01	2.4	15	0	6.25
SS-03	4.8	15	0	3.125
SS-07	2.4	60	0	25
SS-09	4.8	60	0	12.5
SS-14	3.6	37.5	30	10.42
SS-19	2.4	15	60	6.25
SS-21	4.8	15	60	3.125
SS-25	2.4	60	60	25
SS-27	4.8	60	60	12.5

Based on an experimentally well verified modeling method (NCHRP 2005), finite-element analyses of 9 simple-span bridges (32 cases) were conducted using ABAQUS (HKS 2000). Simple-span bridge configurations analyzed are summarized in Table 1. Their main parameters were 15 and 60 m span lengths, 2.4 and 4.8 m girder spacings, and 0 and 60° skew angles. In addition, bridges with intermediate values (e.g., 30° skew angle) were also considered to investigate the effects of intermediate values on effective width.

Bridge FEM models were subjected to the nominal live load, which consists of AASHTO HL-93 trucks and lane load, including impact effects (AASHTO LRFD 2004). Both truck and lane loads were applied at the specific location to simulate the maximum positive moment condition. Longitudinally, the middle axles of the trucks are located at midspan of the bridge, while they were placed transversely across the width to maximize the bending moment in either interior or exterior girders, whichever was the focus of the case.

The effective slab width values were computed along the span using the new definition for positive moment section [Eq. (1)]. Fig. 3 illustrates the effective slab width ratio variation (b_{eff}/b) and associated bending moment diagrams for various locations along the span (expressed as normalized span length x/L) for simple-span bridges, where b =physical slab width, b_{eff} =computed effective width values; x =distance along the span; and L =span length. The values were determined based on the finite-element analysis results taken between a half-width on one side and the other half-width on the other side of the interior girder, and analogously for exterior girders. The bending moments were calculated from element stresses and cross-sectional areas. The small diagrams in each plot show aspect ratio of the bridge and truck load placement locations. The circles on the plot represent the data points which were joined by straight lines. The series of numbers after the bridge identification contain the bridge configuration information. The three numbers are girder spacing (m), span length (m), and skew angle (deg). Effective width values of the most interest are located at midspan sections where maximum bending moments occur. The results in Fig. 3 indicate full slab width as the effective slab width for all nonskewed bridges which lie within the L/S range of 3.125 and 25. For the highly skewed bridges, three out of four bridges exhibit effective slab width ratios of less than 1.0, except the SS-25 bridge which has the largest L/S of 25. Skewed bridges that have small L/S values, such as SS-19 and SS-21, behave differently from what line girder analysis would predict. Instead, they have a two-way plate/beam bending combination which induces transverse bending mo-

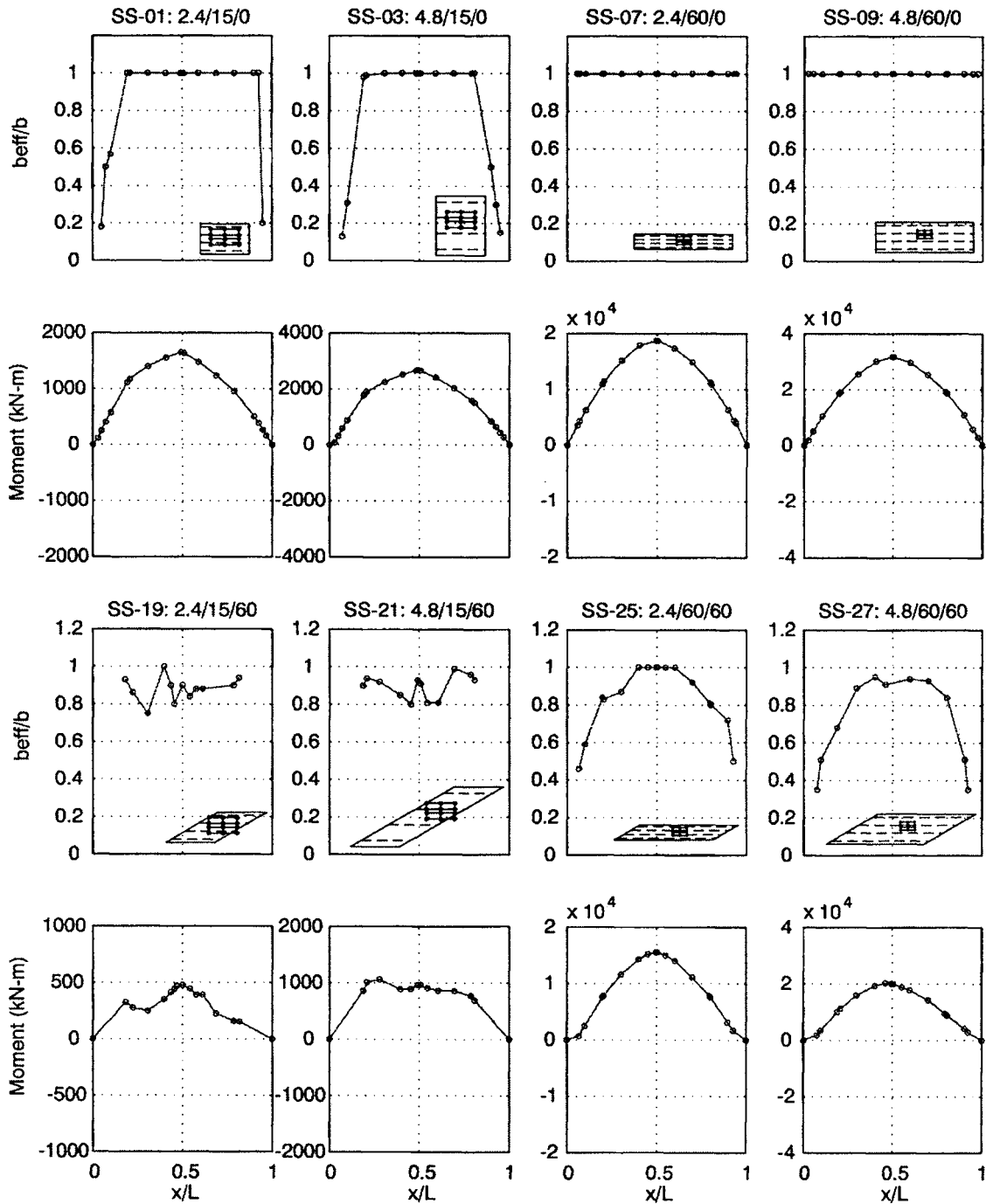


Fig. 3. b_{eff}/b ratio and bending moment versus x/L for simple-span bridges

ment and results in bending moments obtained from FEM that are smaller compared to the line-girder moments. It must be noted that Fig. 3 only shows the results for one particular load case, i.e., positive moment loading at the serviceability (AASHTO-LRFD Service II) limit state. Results from other load cases can be found in NCHRP (2005).

Multiple-Span Continuous Bridges

All three parameters, i.e., S , L , and θ , were also considered in the set of multiple-span continuous bridges along with an additional parameter called span ratio (L_2/L_1) where L_2 and L_1 = interior and exterior span lengths, respectively.

There are four factors ($k=4$) with two levels ($p=2$) for each factor. A total number of factorial cases becomes $p^k=2^4=16$ bridge configurations, which are summarized in Table 2. Their main parameters were 2.4 and 4.8 m girder spacings, 20 and 60 m exterior span lengths, 1.0 and 1.5 interior-to-exterior span ratios, and 0 and 60° skew angles. A total of 192 multiple-span continuous cases were considered. In addition, bridges with intermediate values (e.g., 30° skew angle) were analyzed to investigate the effects of intermediate values on effective width values.

For the negative moment loading, two truck middle axles were placed on the exterior span at $0.6L_1$ and the other two truck middle axles were placed at $1.4L_2$, where L_2 = interior span length.

Table 2. Multiple-Span Continuous Parametric Study Cases

Bridge identification	Parameter				L/S
	S (m)	L ₁ (m)	L ₂ /L ₁	θ (degrees)	
CS-01	2.4	20	1.0	0	8.33
CS-03	4.8	20	1.0	0	4.17
CS-07	2.4	60	1.0	0	25
CS-09	4.8	60	1.0	0	12.5
CS-19	2.4	20	1.5	0	8.33
CS-21	4.8	20	1.5	0	4.17
CS-25	2.4	60	1.5	0	25
CS-27	4.8	60	1.5	0	12.5
CS-41	3.6	40	1.25	30	11.1
CS-55	2.4	20	1.0	60	8.33
CS-57	4.8	20	1.0	60	4.17
CS-61	2.4	60	1.0	60	25
CS-63	4.8	60	1.0	60	12.5
CS-73	2.4	20	1.5	60	8.33
CS-75	4.8	20	1.5	60	4.17
CS-79	2.4	60	1.5	60	25
CS-81	4.8	60	1.5	60	12.5

These locations were systematically chosen based on influence line concepts to maximize the negative bending moment at the interior support. All trucks' rear axles were facing the closest abutment as described for the positive moment loading. Similarly, lane load was applied on both spans where the trucks were located, i.e., Spans 1 and 2.

The main focus of the negative moment loading is on the region close to the interior pier where the negative moment is maximized. Figs. 4 and 5 demonstrate how b_{eff}/b varies in the region close to the interior pier, $1.0L_1$. The small diagrams in each plot show aspect ratios and truck load placement locations on the bridge. In the region over the interior pier ($1.0L_1$), almost all nonskewed bridges experience full width as the effective slab width, except the CS-03 bridge in Fig. 4. Effective width ratios become smaller as sections get closer to the points of inflection. This behavior is very similar to simple-span cases, where the points of inflection analogously represent end-supports where bending moments vanish. Effective width ratios increase back up to unity as sections migrate away from the points of inflection into positive moment regions. Fig. 5 shows that for the case of skewed bridges, there are a few cases which have the effective slab width of smaller than 1.0, especially the ones with short span length and wide girder spacing. Those cases are CS-57, CS-63, and CS-75. In addition, the bending moments associated with these skewed bridges are smaller than the bending moments from the line-girder analysis results. The locations of truck load placement have a major impact on the computed effective slab width ratios, especially in the short and highly skewed bridges, where the tire footprints are not as assumed in the design using line-girder analysis.

In addition, the positive moment loading of multiple-span continuous bridges were also considered in this study by placing the truck middle axles at $0.4L_1$ where L_1 is the exterior span length, with the rear axle facing the closest abutment. All nonskewed bridge results indicate that the full width can be used as the effective slab width for the positive moment section at $0.4L_1$. Due to space limitation, the results are not shown in this paper but can be found in NCHRP (2005).

Effective Width Candidate Design Equations

Effective width candidate design equations were derived by performing regression analyses based on the b_{eff}/b values extracted from the various FEM models in the finite-element parametric study in the vicinity of the maximum positive and negative moment sections (Chiewanichakorn 2005; Chen et al. 2005). The candidate effective width equations for the positive moment section were derived from the results of simple-span bridges, whereas the candidate effective width equations for the negative moment section were derived from the analysis of the multiple span continuous bridges.

Positive Moment Sections

Two different methods were used to derive the effective width candidate design equations for positive moment section. These were designated as—(1) all five values; and (2) interpolation. The *all five values* method used five b_{eff}/b values near midspan at 0.4, 0.45, 0.5, 0.55, and $0.6L$. This method included both L/S and θ parameters. The *interpolation* method assumed b_{eff}/b of 1.0 for all straight bridges and varied b_{eff}/b with skew angle alone.

For positive moment sections, four different sets of proposed design criteria are summarized in the following equations. All candidate design equations were divided into four categories: (1) Interior girder only, (2) exterior girder only, (3) both interior and exterior girders, and (4) full width for both interior and exterior girders:

- *Interior girder only*
All five values

$$\frac{b_{\text{eff}}}{b} = 0.959 + 0.003 \frac{L}{S} - 0.001\theta \quad (4)$$

Interpolation

$$\frac{b_{\text{eff}}}{b} = 1 - \frac{\theta^3}{5 \times 10^5} + \frac{\theta^2}{10^4} - \frac{\theta}{10^3} \quad (5)$$

- *Exterior girder only*
All five values

$$\frac{b_{\text{eff}}}{b} = 0.963 + 0.003 \frac{L}{S} - 0.002\theta \quad (6)$$

Interpolation

$$\frac{b_{\text{eff}}}{b} = 1 - \frac{\theta^3}{10^6} - \frac{\theta^2}{5 \times 10^4} + \frac{\theta}{10^3} \quad (7)$$

- *Both interior and exterior girders*
All five values

$$\frac{b_{\text{eff}}}{b} = 0.961 + 0.003 \frac{L}{S} - 0.002\theta \quad (8)$$

Interpolation

$$\frac{b_{\text{eff}}}{b} = 1 - \frac{\theta^3}{10^6} + \frac{\theta^2}{10^5} + \frac{\theta}{10^4} \quad (9)$$

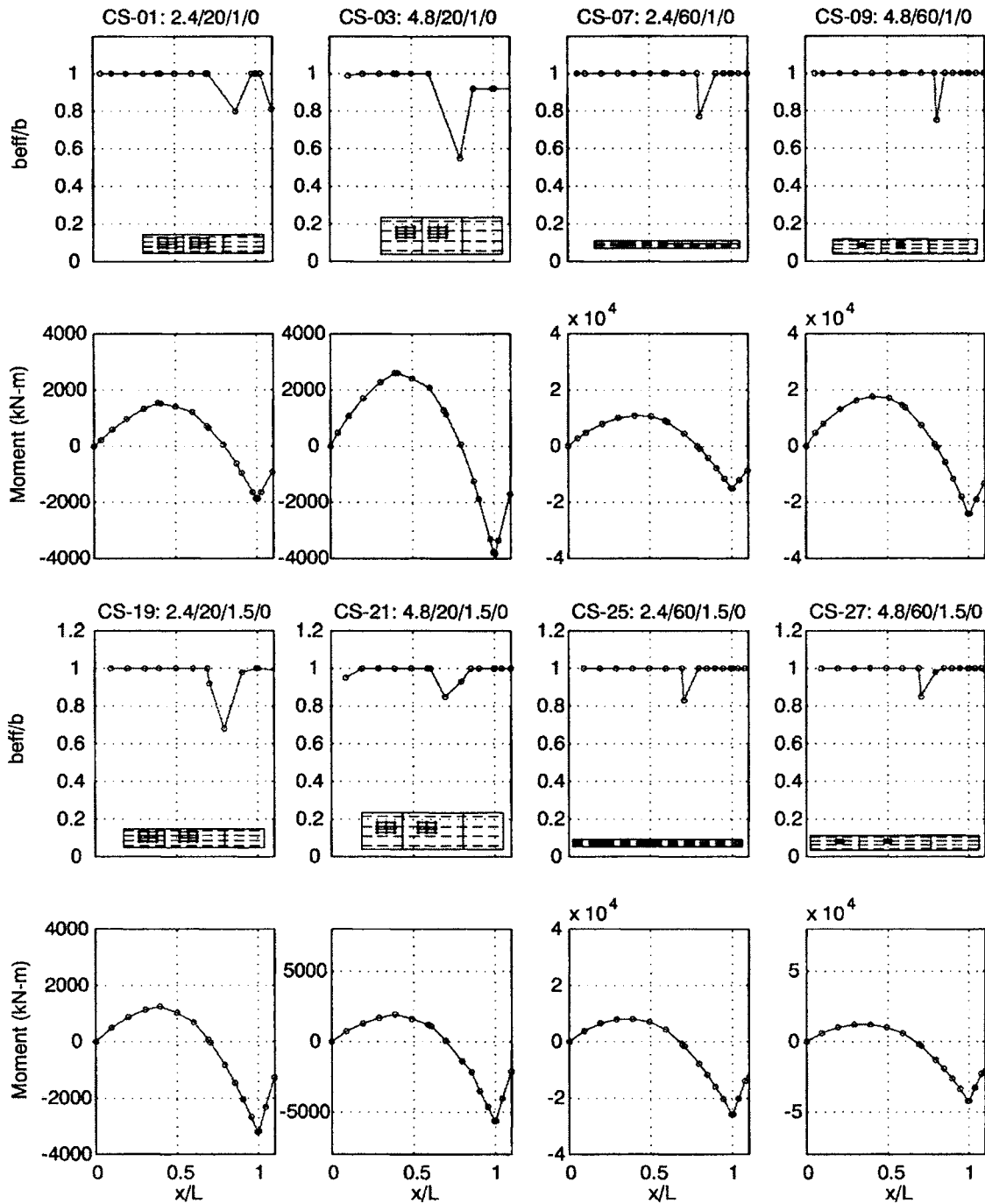


Fig. 4. b_{eff}/b ratio and bending moment versus x/L_1 for multiple-span bridges (nonskewed)

- Full width for both interior and exterior girders

$$\frac{b_{\text{eff}}}{b} = 1 \quad (10)$$

Negative Moment Sections

For negative moment sections, the slab can be divided into two types—namely, uncracked and cracked sections. Effective width ratios (b_{eff}/b) were computed based on the new definition for the negative moment section [Eq. (2)]. Five different sections along

the span near the interior support were considered. The candidate design equations were divided into four categories as described for the positive moment sections. Span ratio (L_2/L_1) was also considered in the candidate design equations. Thirteen candidate design equations were generated as the following equations for negative moment sections:

- Interior girder only
Cracked (with L_2/L_1)

$$\frac{b_{\text{eff}}}{b} = 0.74 + 0.004 \frac{L_1}{S} - 0.002\theta + 0.155 \frac{L_2}{L_1} \quad (11)$$

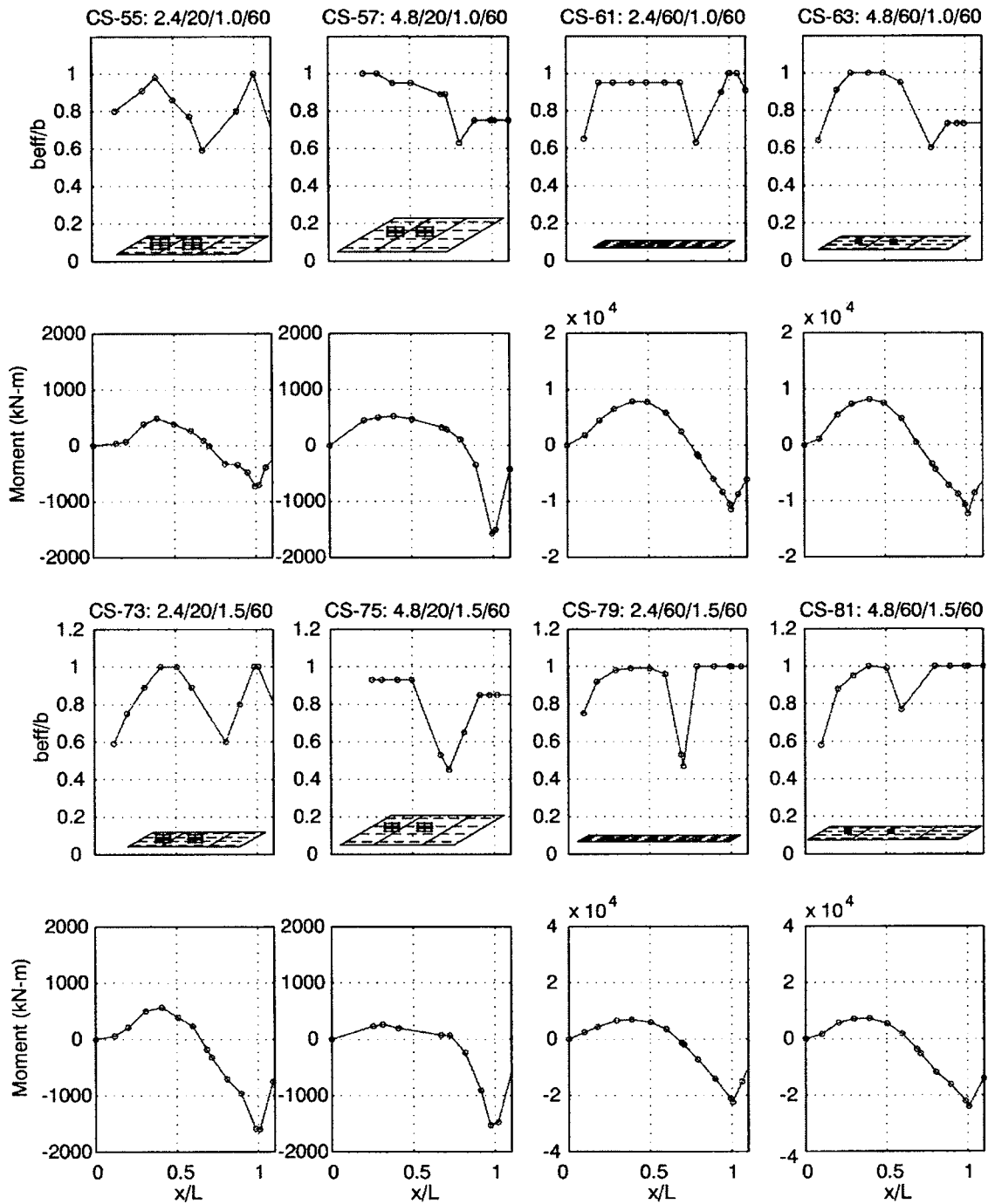


Fig. 5. b_{eff}/b ratio and bending moment versus x/L_1 for multiple span bridges (skewed)

Cracked (without L_2/L_1)

$$\frac{b_{eff}}{b} = 0.933 + 0.004 \frac{L_1}{S} - 0.0020 \quad (12)$$

Uncracked (with L_2/L_1)

$$\frac{b_{eff}}{b} = 0.674 + 0.004 \frac{L_1}{S} - 0.0020 + 0.194 \frac{L_2}{L_1} \quad (13)$$

Uncracked (without L_2/L_1)

$$\frac{b_{eff}}{b} = 0.916 + 0.004 \frac{L_1}{S} - 0.0020 \quad (14)$$

• Exterior girder only
Cracked (with L_2/L_1)

$$\frac{b_{eff}}{b} = 0.885 + 0.002 \frac{L_1}{S} - 0.00020 + 0.063 \frac{L_2}{L_1} \quad (15)$$

Cracked (without L_2/L_1)

$$\frac{b_{eff}}{b} = 0.963 + 0.002 \frac{L_1}{S} - 0.00020 \quad (16)$$

Table 3. Impact Assessment Results of Positive Moment Section at Service II Limit State (Simple Span)

Bridge identification	S (m)	L (m)	θ (degrees)	L/S	p_1 (%)					
					AASHTO	Eq. (4)	Eq. (5)	Eq. (8)	Eq. (9)	Eq. (10)
SS-01	2.4	15	0	6.25	0.00	0.46	0.65	0.46	0.65	0.65
SS-03	4.8	15	0	3.125	0.00	3.30	3.50	3.50	3.50	3.50
SS-07	2.4	60	0	25	0.00	0.25	0.25	0.25	0.25	0.25
SS-09	4.8	60	0	12.5	0.00	3.11	3.11	3.11	3.11	3.11
SS-19	2.4	15	60	6.25	0.00	-0.39	-0.78	-0.78	-1.46	0.58
SS-21	4.8	15	60	3.125	0.00	2.93	2.74	2.64	2.16	3.98
SS-25	2.4	60	60	25	0.00	-0.92	-0.92	-0.33	-1.59	0.33
SS-27	4.8	60	60	12.5	0.00	2.81	2.35	2.53	1.79	3.46

Note: $12t_s$ limitation in current AASHTO governs the effective widths used in the design of all simple-span bridges.

Uncracked (with L_2/L_1)

$$\frac{b_{\text{eff}}}{b} = 0.841 + 0.002 \frac{L_1}{S} - 0.001\theta + 0.090 \frac{L_2}{L_1} \quad (17)$$

Uncracked (without L_2/L_1)

$$\frac{b_{\text{eff}}}{b} = 0.953 + 0.002 \frac{L_1}{S} - 0.001\theta \quad (18)$$

• Both interior and exterior girders

Cracked (with L_2/L_1)

$$\frac{b_{\text{eff}}}{b} = 0.812 + 0.003 \frac{L_1}{S} - 0.001\theta + 0.109 \frac{L_2}{L_1} \quad (19)$$

Cracked (without L_2/L_1)

$$\frac{b_{\text{eff}}}{b} = 0.948 + 0.003 \frac{L_1}{S} - 0.001\theta \quad (20)$$

Uncracked (with L_2/L_1)

$$\frac{b_{\text{eff}}}{b} = 0.757 + 0.003 \frac{L_1}{S} - 0.00142\theta - 0.001 \frac{L_2}{L_1} \quad (21)$$

Uncracked (without L_2/L_1)

$$\frac{b_{\text{eff}}}{b} = 0.953 + 0.003 \frac{L_1}{S} - 0.00145\theta \quad (22)$$

• Full width for both interior and exterior girders

$$\frac{b_{\text{eff}}}{b} = 1 \quad (23)$$

Impact Assessment

In order to select the most appropriate design criteria from the various candidate design equations, a systematic procedure is required. In this paper, the method proposed in the NCHRP 12-50 Project (NCHRP 2003) is employed to investigate the impact of different candidate design equations. The impact assessment was performed based on the *LRFR rating factor* (Minervino et al. 2004).

The proposed method is based on the percentage difference between two outputs from the analyses. It is assumed that two programs, or specification provisions in this study, generate results (stress, moment, etc.) at n points in a girder, which are termed as a_i and b_i ($i=1, 2, \dots, n$), where a and b represent the

two different programs or specification provisions. At each point, the absolute average quantity, m_i , is computed as

$$m_i = \left| \frac{a_i + b_i}{2} \right| \quad (24)$$

The NCHRP 12-50 Project suggested the use of an *absolute average* or p_1 -value as an indicator for measuring impacts, computed as in

$$p_i(\%) = \frac{|a_i + b_i|}{m_i} \times 100 \quad (25)$$

The two results are concluded to be different when p_1 -value is larger than the threshold acceptable percentage (p_{allow}).

Positive Moment Regions

Eight simple-span bridges were selected for impact assessment for the positive moment sections. Table 3 shows impact assessment results for interior girder in terms of absolute average value (p_1) for each candidate effective width criterion and the current AASHTO provisions. The absolute average values were computed relative to the current AASHTO LRFR rating factors. Based on the computed average value, it became apparent that the impact of effective width candidate design equations in the positive moment sections is insignificant. The maximum p_1 -value for the interior girder was 4%, for full width. In addition, Figs. 6(a and b) illustrate the variation of effective width ratio for nonskewed and skewed bridges, respectively. Each curve was calculated based on Eqs. (4), (6), and (8) for "interior," "exterior," and "both," respectively, for 0 and 60° skew angle. The differences (each line representing a different candidate design equation) are insignificant. Fig. 6(c) demonstrates the curves of effective width design equations derived by an interpolation method based on results for bridge with skew angles of 0, 30 and 60° (Chen et al. 2005). These curves were computed from Eqs. (5), (7), and (9) for interior, exterior, and both, respectively. Again, the differences among the three equations are very small.

Negative Moment Regions

Tables 4 and 5 show the absolute average values (p_1) for each candidate effective width design equation for the Service II Limit State in negative moment sections. Tables 6 and 7 show the p_1 values for the Strength I Limit State.

In the negative moment sections, p_1 values for the Service II Limit State were very small (see Tables 4 and 5), which indicate an insignificant change in design stress value in the flange due to

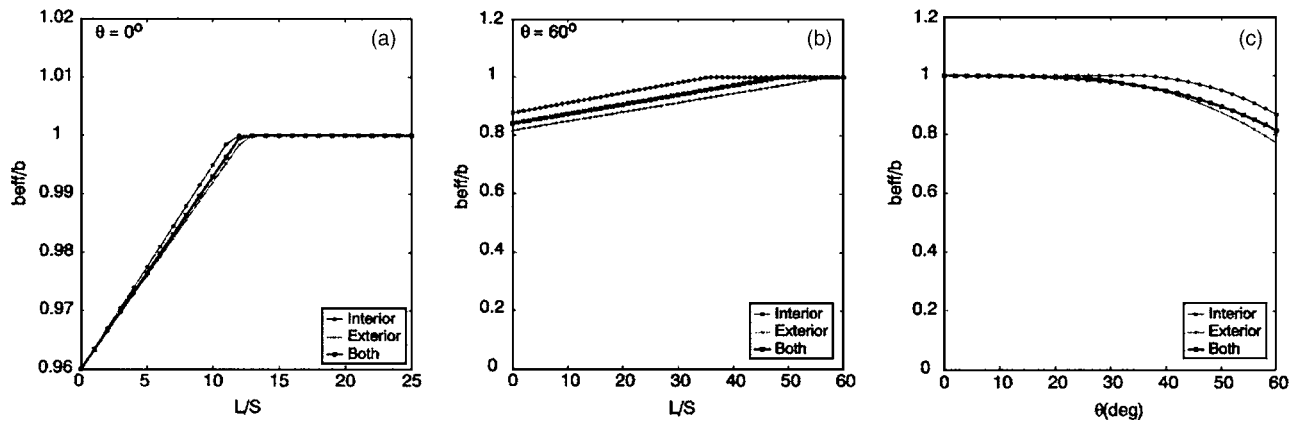


Fig. 6. Proposed design criteria for the positive moment section as (a) function of L/S when $\theta=0^\circ$; (b) function of L/S when $\theta=60^\circ$; and (c) function of θ only

the change of effective width among the candidate effective width design equations. As the result, a full width is an appropriate estimation of effective width in negative moment sections at the serviceability limit state. It must also be noted that the effect of span ratio (L_2/L_1) is negligible. However, some of the Strength I Limit State absolute average values (p_1) show more significant changes as shown in Tables 6 and 7. These are addressed in the next section.

Effective Width Design Criteria

Positive Moment Sections

In the impact assessment, the absolute average percentage values show insignificant differences among all the candidate design equations. The largest p_1 value is less than 4%, which is associated with a full slab width, compared to the current AASHTO-

LRFD code. For simplicity and accuracy considerations, the full slab width is recommended as the proposed design criteria for the positive moment section for compositely designed girders at both service and strength limit states, regardless of skew angle.

Nassif et al. (2005) presents a related study of effective width for slab-on-girder structural configurations. The focus and scope of that study differs somewhat from the study presented herein—particularly in the following aspects: (1) the study does not deal with negative moment regions; (2) it does not address impact assessments; (3) it does not address concrete girders; (4) it does not address skew; (5) the recommended deviation from full width is based on a limited sample size that is not representative of the vast majority of girder bridge configurations anyway; and (6) the field-test inferred results are dependent on assumed value of n and are based largely on configurations where AASHTO, which is conservative, would currently allow full width anyway.

In spite of its limitations, however, the effort by Nassif et al.

Table 4. Impact Assessment Results of Negative Moment Section at Service II Limit State (without L_2/L_1)

Bridge identification	S (m)	L (m)	L_2/L_1	θ (degrees)	L_1/S	p_1 (%)					
						AASHTO	Eq. (12)	Eq. (14)	Eq. (20)	Eq. (22)	Eq. (23)
CS-01 ^a	2.4	20	1.0	0	8.33	0.00	-0.06	0.00	-0.06	0.00	-0.06
CS-03 ^a	4.8	20	1.0	0	4.17	0.00	0.00	0.00	0.00	0.00	0.00
CS-07 ^b	2.4	60	1.0	0	25	0.00	-0.55	-0.55	-0.55	-0.55	-0.55
CS-09 ^b	4.8	60	1.0	0	12.5	0.00	-0.06	-0.06	-0.06	-0.06	-0.06
CS-19 ^b	2.4	20	1.5	0	8.33	0.00	-0.06	0.00	0.00	0.00	-0.06
CS-21 ^a	4.8	20	1.5	0	4.17	0.00	-0.33	-0.33	-0.33	-0.33	-0.33
CS-25 ^b	2.4	60	1.5	0	25	0.00	0.03	0.03	0.03	0.03	0.03
CS-27 ^b	4.8	60	1.5	0	12.5	0.00	0.14	0.14	0.14	0.14	0.14
CS-55 ^a	2.4	20	1.0	60	8.33	0.00	0.11	0.11	0.05	0.05	0.00
CS-57 ^a	4.8	20	1.0	60	4.17	0.00	0.06	0.00	0.06	0.06	0.18
CS-61 ^b	2.4	60	1.0	60	25	0.00	0.00	0.00	0.00	0.00	0.00
CS-63 ^b	4.8	60	1.0	60	12.5	0.00	0.04	0.00	0.04	0.04	0.04
CS-73 ^b	2.4	20	1.5	60	8.33	0.00	0.06	0.06	0.00	0.06	-0.06
CS-75 ^a	4.8	20	1.5	60	4.17	0.00	0.11	0.06	0.11	0.11	0.17
CS-79 ^b	2.4	60	1.5	60	25	0.00	-0.06	-0.12	-0.03	-0.06	0.06
CS-81 ^b	4.8	60	1.5	60	12.5	0.00	0.23	0.23	0.27	0.27	0.32

^a $L/4$ limitation governs the effective width used in the design of this bridge.

^b $12t_s$ limitation in current AASHTO governs the effective width used in the design of this bridge.

Table 5. Impact Assessment Results of Negative Moment Section at Service II Limit State (with L_2/L_1)

Bridge identification	S (m)	L (m)	L_2/L_1	θ (degrees)	L_1/S	P_1 (%)					
						AASHTO	Eq. (11)	Eq. (13)	Eq. (19)	Eq. (21)	Eq. (23)
CS-01 ^a	2.4	20	1.0	0	8.33	0.00	0.00	0.00	0.00	0.18	-0.06
CS-03 ^a	4.8	20	1.0	0	4.17	0.00	0.00	0.00	0.00	-0.05	0.05
CS-07 ^b	2.4	60	1.0	0	25	0.00	-0.55	0.00	0.00	-0.05	-0.55
CS-09 ^b	4.8	60	1.0	0	12.5	0.00	-0.06	-0.06	-0.06	0.00	-0.06
CS-19 ^b	2.4	20	1.5	0	8.33	0.00	-0.06	-0.06	-0.06	0.24	-0.06
CS-21 ^a	4.8	20	1.5	0	4.17	0.00	-0.33	-0.33	-0.33	-0.20	-0.33
CS-25 ^b	2.4	60	1.5	0	25	0.00	0.03	0.03	0.03	-0.22	0.03
CS-27 ^b	4.8	60	1.5	0	12.5	0.00	0.14	0.14	0.14	0.07	0.14
CS-55 ^a	2.4	20	1.0	60	8.33	0.00	0.16	0.16	0.05	0.33	0.00
CS-57 ^a	4.8	20	1.0	60	4.17	0.00	0.00	0.00	0.06	0.00	0.18
CS-61 ^b	2.4	60	1.0	60	25	0.00	0.00	0.00	0.00	-0.05	0.00
CS-63 ^b	4.8	60	1.0	60	12.5	0.00	0.00	0.00	0.04	0.00	0.04
CS-73 ^b	2.4	20	1.5	60	8.33	0.00	0.00	0.06	0.00	0.17	-0.06
CS-75 ^a	4.8	20	1.5	60	4.17	0.00	0.11	0.11	0.11	0.00	0.11
CS-79 ^b	2.4	60	1.5	60	25	0.00	0.00	-0.03	0.03	-0.43	0.06
CS-81 ^b	4.8	60	1.5	60	12.5	0.00	0.27	0.27	0.27	0.05	0.32

^a $L/4$ limitation governs the effective width used in the design of this bridge.

^b $12t_s$ limitation in current AASHTO governs the effective width used in the design of this bridge.

(2005) provides independent confirmation that, over the range of parameters it shares with the study presented herein, its recommended effective width criteria is the same as that presented herein, i.e., full width.

Negative Moment Sections

In order to choose the most appropriate equation from the thirteen possible equations, the selection process would need to be effective and built on a sound basis. Thus, we consider the following categories of factors.

Cracked versus Uncracked

The analysis results show that cracking takes place at the maximum negative moment section or $1.0L_1$ at service loads. In addition, cracking of the slab increases the effective width which induces larger compressive stresses in the bottom flange of the girders. There are six candidate design equations derived for cracked slab sections as shown in Table 8.

Criteria for Interior, Exterior, and Both Girders

Two of the six candidate design equations for cracked sections pertain to interior girder only, two equations pertain to exterior

Table 6. Impact Assessment Results of Negative Moment Section at Strength I Limit State (without L_2/L_1)

Bridge identification	S (m)	L (m)	L_2/L_1	θ (degrees)	L_1/S	P_1 (%)					
						AASHTO	Eq. (12)	Eq. (14)	Eq. (20)	Eq. (22)	Eq. (23)
CS-01 ^b	2.4	20	1.0	0	8.33	0.00	0.86	0.29	0.86	0.58	0.29
CS-03 ^b	4.8	20	1.0	0	4.17	0.00	14.30	14.14	14.30	14.30	14.62
CS-07 ^a	2.4	60	1.0	0	25	0.00	0.43	0.43	0.43	0.43	0.43
CS-09 ^a	4.8	60	1.0	0	12.5	0.00	-45.9	-46.2	-45.9	-45.9	-45.5
CS-19 ^b	2.4	20	1.5	0	8.33	0.00	-7.89	0.27	-7.89	0.55	1.45
CS-21 ^a	4.8	20	1.5	0	4.17	0.00	-30.5	-37.7	-29.8	-30.5	-27.4
CS-25 ^b	2.4	60	1.5	0	25	0.00	0.08	0.08	0.08	0.08	0.08
CS-27 ^b	4.8	60	1.5	0	12.5	0.00	-2.45	-2.35	-2.45	-2.45	-2.65
CS-55 ^a	2.4	20	1.0	60	8.33	0.00	-2.23	-3.19	-0.79	-1.66	1.71
CS-57 ^a	4.8	20	1.0	60	4.17	0.00	2.44	2.15	3.02	2.63	4.44
CS-61 ^b	2.4	60	1.0	60	25	0.00	0.23	0.38	0.08	0.23	-0.15
CS-63 ^b	4.8	60	1.0	60	12.5	0.00	6.78	5.83	8.04	7.10	10.58
CS-73 ^b	2.4	20	1.5	60	8.33	0.00	-1.06	-2.22	-0.10	-0.29	0.00
CS-75 ^a	4.8	20	1.5	60	4.17	0.00	-30.9	-31.1	-30.6	-30.8	-30.1
CS-79 ^b	2.4	60	1.5	60	25	0.00	-0.33	-0.49	-0.08	-0.33	0.16
CS-81 ^b	4.8	60	1.5	60	12.5	0.00	0.26	0.35	0.09	0.26	-0.17

^a $L/4$ limitation governs the effective width used in the design of this bridge.

^b $12t_s$ limitation in current AASHTO governs the effective width used in the design of this bridge.

Table 7. Impact Assessment Results of Negative Moment Section at Strength I Limit State (with L_2/L_1)

Bridge identification	S (m)	L (m)	L_2/L_1	θ (degrees)	L_1/S	p_1 (%)					
						AASHTO	Eq. (11)	Eq. (13)	Eq. (19)	Eq. (21)	Eq. (23)
CS-01 ^a	2.4	20	1.0	0	8.33	0.00	-0.19	-0.68	0.29	-4.32	0.29
CS-03 ^a	4.8	20	1.0	0	4.17	0.00	13.97	13.89	14.14	11.75	14.62
CS-07 ^b	2.4	60	1.0	0	25	0.00	0.43	0.00	0.09	-1.21	0.43
CS-09 ^b	4.8	60	1.0	0	12.5	0.00	-46.7	-47.4	-46.5	3.03	-45.5
CS-19 ^b	2.4	20	1.5	0	8.33	0.00	1.45	1.45	1.45	-3.63	1.45
CS-21 ^a	4.8	20	1.5	0	4.17	0.00	28.1	-28.6	-28.1	5.99	-27.4
CS-25 ^b	2.4	60	1.5	0	25	0.00	0.08	0.08	0.08	-0.75	0.08
CS-27 ^b	4.8	60	1.5	0	12.5	0.00	-2.65	-2.65	-2.65	-0.68	-2.65
CS-55 ^a	2.4	20	1.0	60	8.33	0.00	-3.44	-4.75	-1.35	-7.25	1.71
CS-57 ^a	4.8	20	1.0	60	4.17	0.00	2.05	1.57	2.73	0.59	4.44
CS-61 ^b	2.4	60	1.0	60	25	0.00	1.57	1.20	0.23	0.38	-0.15
CS-63 ^b	4.8	60	1.0	60	12.5	0.00	5.51	4.30	7.41	1.51	10.58
CS-73 ^b	2.4	20	1.5	60	8.33	0.00	-0.10	-0.29	0.00	-7.33	0.00
CS-75 ^a	4.8	20	1.5	60	4.17	0.00	-30.7	-30.8	-30.4	-37.1	-30.1
CS-79 ^b	2.4	60	1.5	60	25	0.00	-0.08	-0.16	0.08	-1.24	0.16
CS-81 ^b	4.8	60	1.5	60	12.5	0.00	0.09	0.26	0.00	0.43	-0.17

^a $L/4$ limitation governs the effective width used in the design of this bridge.

^b $12t_s$ limitation in current AASHTO governs the effective width used in design of this bridge.

girders only, and two equations are derived for both interior and exterior girders data. The p_1 -values indicate insignificant differences among all these equations for the Service II Limit State (Tables 4 and 5).

The Strength I Limit State governs the design of the negative moment section for these bridges. The p_1 values indicate that all six candidate design equations can be as unconservative as 47% compared to the current specifications. The changes were most significant when all of the following conditions are met: (1) large girder spacing (4.8 m), (2) the girder section is compact based on current AASHTO, and (3) the same girder section is noncompact based on proposed new full-width provisions proposed herein.

Table 8. Selection Criteria of Effective Width for the Negative Moment Section

Stages	Equation number	L/S
Cracked section	(11)	$\frac{b_{\text{eff}}}{b} = 0.74 + 0.004 \frac{L_1}{S} - 0.002\theta + 0.155 \frac{L_2}{L_1}$
	(12)	$\frac{b_{\text{eff}}}{b} = 0.933 + 0.004 \frac{L_1}{S} - 0.002\theta$
	(15)	$\frac{b_{\text{eff}}}{b} = 0.885 + 0.002 \frac{L_1}{S} - 0.0002\theta + 0.063 \frac{L_2}{L_1}$
	(16)	$\frac{b_{\text{eff}}}{b} = 0.963 + 0.002 \frac{L_1}{S} - 0.0002\theta$
	(19)	$\frac{b_{\text{eff}}}{b} = 0.812 + 0.003 \frac{L_1}{S} - 0.001\theta + 0.109 \frac{L_2}{L_1}$
	(20)	$\frac{b_{\text{eff}}}{b} = 0.948 + 0.003 \frac{L_1}{S} - 0.001\theta$
Both girders	(19)	$\frac{b_{\text{eff}}}{b} = 0.812 + 0.003 \frac{L_1}{S} - 0.001\theta + 0.109 \frac{L_2}{L_1}$
	(20)	$\frac{b_{\text{eff}}}{b} = 0.948 + 0.003 \frac{L_1}{S} - 0.001\theta$
Without L_2/L_1	(20)	$\frac{b_{\text{eff}}}{b} = 0.948 + 0.003 \frac{L_1}{S} - 0.001\theta$

The combinations of the above factors lead to the greatest effect on the change of effective width provisions because larger effective width raises the neutral axis upward and flexural resistance provisions for noncompact sections in AASHTO were based on a limiting flange stress and elastic behavior, whereas compact sections utilize up to full plastic moment capacity. This substantial impact does not compromise the proposed criteria since probably no existing bridges in the nationwide inventory have the attributes of wide girder spacings as well as composite design with compact webs in the negative moment region.

The p_1 values show minor differences among all six equations. Thus, having one equation for both interior and exterior girders would not be inaccurate. Hence, two out of the six candidate design equations were chosen, which were Eqs. (19) and (20) (see Table 8).

With Span Ratio and without Span Ratio

There are only two design equations remaining in this selection process, one with L_2/L_1 and one without L_2/L_1 . The differences between the two design equations are insignificant. Therefore, the span ratio parameter can be disregarded from the design equation for simplicity purposes.

It is clear from p_1 values in the last column representing full slab width [designated as Eq. (23)] in Tables 4–7 that full slab width exhibits similar impact assessment compared to other design equations. Thus, the simplest proposed design criterion for the negative moment sections is full width, although a slightly more accurate expression can be obtained from Eq. (20) (see Table 8).

Range of Applicability

As the proposed effective width design criteria for both positive and negative moment sections were derived based on the results of parametric study, that study's range of applicability should be noted: $L \leq 60$ m, $S \leq 4.8$ m, and $\theta \leq 60^\circ$. Its results, however, suggest that full effective width is more readily obtained for longer spans; thus spans longer than 60 m could reasonably utilize the full width as effective.

The proposed design criteria were validated with both conventional steel-concrete composite bridges and other types of bridges, i.e., hybrid steel bridges, two-girder bridges with wide girder spacings and either conventional or prestressed slabs, precast/prestressed concrete bulb-tee girder bridges, and steel tub-girder bridges (NCHRP 2005). The results of these cases are not presented in this paper, although they corroborate its results.

For concrete girder bridges as for bridges with wide girder spacing (up to 7.68 m), the design criteria in Eq. (20) or (23) may be utilized. However, there were a limited number of bridges that were investigated during the validation process. Caution must be exercised by the designer regarding the possible use of the criteria with wider girder spacing bridges outside the range of applicability.

Conclusions

A finite-element-based parametric study was performed to derive a proposed simplified design equation to compute effective widths in both positive and negative moment regions. Design of experiment concepts were employed in selecting cases to conduct the parametric study in such a way as to eliminate human bias and therefore create a viable statistical sample. Two types of bridges were considered: Simple-span and multiple-span continuous (3 spans). Three main parameters were considered for simple-span bridges, namely girder spacing (S), span length (L), and skew angle (θ). An additional parameter, span ratio (L_2/L_1), was introduced for the multiple span continuous bridges.

All simple-span bridges exhibit full effective width at all cross sections of practical interest, except the ones with short spans, wide girder spacing, and highly skewed supports. Almost all non-skewed multiple span continuous bridges similarly exhibit full width as the effective width. Those with high skew angle produce smaller effective width.

Several candidate design equations were derived by a regression analysis based on the FEM-extracted results. By performing an impact assessment, the final proposed design criteria were systematically selected.

The full slab width was recommended as the proposed design criterion for the positive moment section for compositely designed girders. As such, bridges with wider girder spacings would have their effective width more significantly liberalized than those with narrower girder spacings. For example, for the bridges in this study with $S=2.4$ m effective width would be increased from $12t_s=2.1$ m to 2.4 m, whereas for the bridges with $S=4.8$ m effective width would be increased from $12t_s=2.9$ m to 4.8 m. The influence on flexural performance ratios is favorable, but relatively small, on the order of 4% or less in a design comparison study (Chen et al. 2005).

The final proposed design criterion for the negative moment section is also full width, although a slightly more accurate expression can be obtained from Eq. (20) and that is,

$$\frac{b_{\text{eff}}}{b} = 0.948 + 0.003 \frac{L_1}{S} - 0.0010$$

Acknowledgments

This work was sponsored by the American Association of State Highway and Transportation Officials, in cooperation with the

Federal Highway Administration, and was conducted in the National Cooperative Highway Research Program, which is administered by the Transportation Research Board of the National Research Council. The opinions and conclusions expressed or implied in this paper are those of the writers. They are not necessarily those of the Transportation Research Board, the National Research Council, the Federal Highway Administration, the American Association of State Highway and Transportation Officials, or the individual states participating in the National Cooperative Highway Research Program.

References

- Adekola, A. O. (1968). "Effective widths of composite beams of steel and concrete." *Struct. Eng.*, 46(9), 285–289.
- Ahn, I., Nottis, A., Chiewanichakorn, M., Carpenter, J., Chen, S., and Aref, A. (2005). "Experimental study of the ultimate behavior at the negative moment regions of composite bridge." *84th Annual Meeting of the Transportation Research Board*, Washington, D.C., Paper 05-2616.
- Ahn, I.-S., Chiewanichakorn, M., Chen, S. S., and Aref, A. J. (2004). "Effective flange width provisions for composite steel bridges." *Eng. Struct.*, 26(12), 1843–1851.
- American Association of State Highway Officials (AASHTO). (1944). *Standard specifications for highway bridges*, 4th Ed., Washington, D.C.
- AASHTO. (2004). *AASHTO-LRFD bridge design specifications*, 3rd Ed., Washington, D.C.
- American Concrete Institute (ACI). (1917). "Proposed standard building regulations for the use of reinforced concrete." *ACI J.*, 13(2), 416.
- ANATECH, Corp. (1997). *ANACAP-U concrete analysis program user's manual*, version 2.5, San Diego.
- Ansourian, P. (1983). "The effective width of continuous beams." *Civil Engineering Transitions*, 25(1), 63–70.
- Aref, A. J., Chiewanichakorn, M., Chen, S. S., and Ahn, I.-S. (2006). "Effective slab width definition for negative moment regions of composite bridges." *J. Bridge Eng.*, in press.
- British Standards Institution (BSI). (1979). "Code of practice for design of composite bridges." *BS 5400 steel, concrete, and composite bridges*, Part 5, London.
- British Standards Institution (BSI). (1982). "Code of practice for design of steel bridges." *BS 5400 steel, concrete, and composite bridges*, Part 3, London.
- Canadian Standards Association (CSA). (2000). "Canadian highway bridge design code." *CAN/CSA-S6-00*, CSA International, Rexdale, Ont., Canada.
- Canadian Standards Association (CSA). (2001). "Commentary on CAN/CSA-S6-00, Canadian Highway Bridge Design Code." CSA International, Rexdale, Ont., Canada.
- Chen, S. S., Aref, A. J., Ahn, I.-S., and Chiewanichakorn, M. (2005). "Effective flange width provisions for composite steel bridges." *Proc., Int. Bridge Conf., Engineers' Society of Western Pennsylvania*, Pittsburgh, Paper IBC 05–23.
- Chen, S. S., Aref, A. J., Ahn, I.-S., Chiewanichakorn, M., Carpenter, J. A., Nottis, A., and Kalpakidis, I. (2005). "Effective slab width for composite steel bridge members." *NCHRP Rep. No. 543*, Transportation Research Board, National Research Council, Washington, D.C.
- Cheung, M. S., and Chan, M. Y. T. (1978). "Finite strip evaluation of effective flange width of bridge girders." *Can. J. Civ. Eng.*, 5(2), 174–185.
- Chiewanichakorn, M. (2005). "Intrinsic method of effective flange width evaluation for steel-concrete composite bridges." Ph.D. dissertation, Univ. at Buffalo–State Univ. of New York, Buffalo, N.Y.
- Chiewanichakorn, M., Aref, A. J., Chen, S. S., and Ahn, I.-S. (2004). "Effective flange width definition for steel-concrete composite bridge girder." *J. Struct. Eng.*, 130(12), 2016–2031.

- Chiewanichakorn, M., Aref, A. J., Chen, S. S., Ahn, I.-S., and Carpenter, J. A. (2005). "Effective flange width of composite girders in negative moment region." *6th Int. Bridge Engineering Conf.*, Transportation Research Board, Boston.
- Committee on Reinforced Concrete Bridges and Culverts. (1916). "Preliminary report." *ACI J.*, 12, 419.
- Daniels, J. H., and Fisher, J. W. (1966). "Shear connector design for highway bridges: Static behavior of continuous composite beams." *Fritz Engineering Laboratory Rep. No. 324.2*, Lehigh Univ., Bethlehem, Pa.
- Elhebaway, M., Fu, C. C., Sahin, M. A., and Schelling, D. R. (1999). "Determination of slab participation from weigh-in-motion bridge testing." *J. Bridge Eng.*, 4(3), 165–173.
- Ferro-Concrete. (1910). *Engineering: An Illustrated Weekly J.*, 90, 607.
- Goldbeck, A. T., and Smith, E. B. (1916). "Test of large reinforced concrete slabs." *ACI J.*, 12(2), 324–333.
- Goode, R. D. (1999). "The Tagushi approach to fractional factorial experimental design." *J. Validation Technology*, 7(1), 443–447.
- Heins, C. P., and Fan, H. M. (1976). "Effective composite beam width at ultimate load." *J. Struct. Div.*, 102(11), 2163–2179.
- Hibbitt, Karlsson and Sorensen, Inc. (HKS). (2000). *ABAQUS/standard user's manual, version 6.1*, Pawtucket, R.I.
- Johnson, R. P., and Anderson, D. (1993). *Designer's handbook to Eurocode 4 (Part 1.1: Design of composite steel and concrete structures)*, Thomas Telford, London.
- Kathol, S., Azizinamini, A., and Luedke, J. (1995). "Strength capacity of steel girder bridges." *Technical Rep.*, Nebraska Department of Roads (NDOR), Lincoln, Neb.
- Minervino, C., Sivakumar, B., Moses, F., Mertz, D., and Edberg, W. (2004). "New AASHTO guide manual for load and resistance factor rating of highway bridges." *J. Bridge Eng.*, 9(1), 43–54.
- Moffatt, K. R., and Dowling, P. J. (1978). "British shear lag rules for composite girders." *J. Struct. Div.*, 104(7), 1123–1130.
- Montgomery, D. C. (2001). *Design and analysis of experiments*, 5th Ed., Wiley, New York.
- Nassif, H. N., Abu-Amra, T., and El-Tawil, S. (2005). "Effective flange width criteria for composite steel girder bridges." *Transportation Research Board 84th Annual Meeting*, Paper No. 05-2477, Washington, D.C.
- National Cooperative Highway Research Program (NCHRP). (2003). "Bridge software-validation guideline and examples." *NCHRP Rep. No. 454*, Transportation Research Board, Washington, D.C.
- National Cooperative Highway Research Program (NCHRP). (2005). "Effective slab width for composite steel bridge members." *NCHRP Rep. No. 543*, Transportation Research Board, Washington, D.C.
- Oehlers, D. J., and Coughlan, C. G. (1986). "The shear stiffness of stud shear connections in composite beams." *J. Constr. Steel Res.*, 6(4), 273–284.
- Special Committee on Concrete and Reinforced Concrete. (1916). "Final report." *Proc. Am. Soc. Civ. Eng.*, 42,(10) 1657–1708.
- Unwin, W. C. (1911). "Simplification of formula for ferro-concrete beams with single reinforcement." *Engineering: An Illustrated Weekly J.*, 91, 267–268.
- Viest, I. M., Fountain, R. S., and Siess, C. P. (1958). "Development of the new AASHO specification for composite steel and concrete bridges." *Bulletin of the National Research Council No. 174*, U.S. Highway Research Board, Washington, D.C., 1–17.
- Viest, I. M., and Siess, C. P. (1953). "Composite construction for I-beam bridges." *Bulletin of the National Research Council*, Vol. 32, No. 161, U.S. Highway Research Board, Washington, D.C., 161–179.
- Waldram, P. J. (1913). "Some notes on the proposed L.C.C. regulations for reinforced concrete—No. II." *Engineering: An Illustrated Weekly J.*, 95, 836–838.
- Welch, K. A. (2003). "Validation of checkweighers: A case study." *J. Validation Technology*, 9(3), 246–252.